



# Experimental identification of force radiation modes

Yamaguchi, Zenzo  
Sakagami, Kimihiro  
Morimoto, Masayuki  
Bolton, J. Stuart

---

(Citation)

Noise Control Engineering Journal, 61(1):81-86

(Issue Date)

2013-01-01

(Resource Type)

journal article

(Version)

Version of Record

(URL)

<https://hdl.handle.net/20.500.14094/90001754>



# Experimental identification of force radiation modes

Zenzo Yamaguchi<sup>a)</sup>, Kimihiro Sakagami<sup>b)</sup>, Masayuki Morimoto<sup>b)</sup> and J. Stuart Bolton<sup>c)</sup>

(Received: 3 July 2012; Revised: 22 January 2013; Accepted: 22 January 2013)

**The location of a vibration source within a machine is sometimes found to have a significant impact upon the machine's radiated sound power. Radiation mode analysis is known to be a powerful tool for interpreting and predicting sound radiation from a vibrating object since radiation modes are independent of a structure's surface vibration. However, knowledge of the radiation modes alone cannot be used directly to understand the relationship between vibration source location and sound power radiation. Previously, it was suggested that the radiation mode concept could be extended to understand the relationship between the sound power and the driving force distribution by combining a structure's mobility matrix and its radiation modes to form force radiation modes ( $f_{\text{rad}}$ -modes). It was demonstrated by simulation that the radiated sound power can be reduced by choosing the driving force location to be at or near the nodes of the force radiation modes. Here, to further validate the usefulness of the force radiation mode concept, the acoustic transfer vectors and the mobility matrix of a thin steel strip mounted in a rigid baffle were first measured. Then, the force radiation modes were calculated by using the experimental data and it was confirmed that the force radiation modes can serve as a practical guide for choosing a vibration source location that minimizes the radiated sound power, especially at low frequencies. © 2012 Institute of Noise Control Engineering.**

Primary subject classification: 74.6; Secondary subject classification: 23.1

## 1 INTRODUCTION

The location of a vibration source within a machine is sometimes found to have a significant impact on its radiated sound power. In practice, treatments based on vibration modal analysis are often applied in an attempt to reduce the sound power radiated by a structure since that approach is simple. However, it is known that the simple reduction of vibration does not always reduce the sound power radiated by a structure<sup>1,2</sup> and that the sound radiation characteristics of a structure must be taken into account when designing a structure for minimum sound power radiation.

One way to account for a structure's sound radiation characteristics is through the use of radiation modes. Radiation mode analysis has been developing since

the early 1990s mainly in the field of Active Noise Control<sup>3,4</sup>; this style of analysis is known to provide a powerful tool for interpreting sound radiation since radiation modes depend only on the shape of the vibrating object and near-by reflecting objects. That is, radiation modes are independent of the spatial distribution of a structure's surface vibration. Recently, radiation mode analysis has been applied to a number of practical subjects<sup>5,6</sup>. By calculating the radiation modes, the surface vibration velocity distribution patterns that radiate sound effectively can be identified. However, knowledge of the radiation modes alone cannot be used directly to understand the relationship between vibration source location and sound power radiation.

In an earlier article, it was shown that the radiation mode concept can be extended to understand the relationship between the sound power and the driving force distribution<sup>7</sup>. In particular, it was demonstrated by simulation that the sound power radiated by a structure can be reduced by moving the driving force location to the nodes of the extended radiation modes (i.e., the force radiation, or  $f_{\text{rad}}$ -modes) even when the overall vibration level is increased by that change<sup>7</sup>. The advantage of using  $f_{\text{rad}}$ -modes is that we can identify the driving force location that will minimize the radiated sound

<sup>a)</sup> Mechanical Engineering Research Laboratory, Kobe Steel, Ltd., 1-5-5 Takatsukada, Nishi-ku, Kobe Hyogo, 651-2271 JAPAN; email: yamaguchi.zenzo@kobeico.com.

<sup>b)</sup> Environmental Acoustics Laboratory, Graduate School of Engineering, Kobe University, Rokko, Nada, Kobe 657-8501 JAPAN.

<sup>c)</sup> Ray W. Herrick Laboratories, School of Mechanical Engineering, Purdue University, 140 S. Martin Jischke Drive, West Lafayette IN 47907-2031 USA.

power without the need to iteratively locate the vibration source at every possible location.

In the work described in this paper, the  $f_{\text{rad}}$ -modes of a vibrating structure were identified by using experimental data only in order to verify the usefulness of the radiation mode concept in guiding noise control design.

## 2 FORCE RADIATION MODES

The sound pressure created by a vibrating structure,  $p$ , can be calculated as the product of the acoustic transfer vector (a row vector),  $\mathbf{Z}$ , and the vibration velocity vector (a column vector) on the boundary,  $\mathbf{v}_e$ : i.e.,

$$p = \mathbf{Z}\mathbf{v}_e. \quad (1)$$

The sound power can then be calculated from a knowledge of the far-field sound pressure,  $p_r$ , where the subscript  $r$  denotes a point on a recovery surface that surrounds the sound source in the far field and which is divided into  $N_{re}$  segments: i.e.,

$$W = \sum_{r=1}^{N_{re}} \frac{|p_r|^2}{2\rho c} S_r = \sum_{r=1}^{N_{re}} \frac{p_r^* p_r}{2\rho c} S_r \quad (2)$$

where  $\rho$  is the ambient fluid density,  $c$  is the speed of sound,  $*$  denotes conjugation and  $S_r$  is the area of each element on the recovery surface. Then, the sound power is obtained by substituting Eqn. (1) into Eqn. (2): i.e.,

$$W = \sum_{r=1}^{N_{re}} \frac{\mathbf{v}_e^H \mathbf{Z}_r^H \mathbf{Z}_r \mathbf{v}_e}{2\rho c} S_r = \mathbf{v}_e^H \mathbf{R} \mathbf{v}_e \quad (3)$$

where  $\mathbf{R}$  is known as the radiation resistance matrix. The eigenvectors of the radiation resistance matrix are the radiation modes.

In addition, the vibration velocities on the boundary can be expressed as the product of the structure's mobility matrix,  $\mathbf{T}$ , and the driving force distribution,  $\mathbf{f}_e$ : i.e.,

$$\mathbf{v}_e = \mathbf{T}\mathbf{f}_e. \quad (4)$$

The average mean square vibration velocity is then:

$$\frac{1}{2N_e} \mathbf{v}_e^H \mathbf{v}_e = \frac{1}{2N_e} \mathbf{f}_e^H \mathbf{T}^H \mathbf{T} \mathbf{f}_e = \frac{1}{2N_e} \mathbf{f}_e^H \mathbf{U} \mathbf{f}_e \quad (5)$$

where  $N_e$  is the total number of elements on the beam. The vibration modes themselves can be obtained from  $\mathbf{U} = \mathbf{T}^H \mathbf{T}$  by executing an eigenvalue/eigenvector decomposition.

By substituting Eqn. (4) into Eqn. (3), the driving forces can be separated from both the sound field and the structure: i.e.,

$$W = \mathbf{f}_e^H \mathbf{T}^H \mathbf{R} \mathbf{T} \mathbf{f}_e = \mathbf{f}_e^H \mathbf{C} \mathbf{f}_e \quad (6)$$

where  $\mathbf{C}$  is real, symmetric and positive definite. As a result of the latter properties,  $\mathbf{C}$  possesses an eigenvalue/eigenvector decomposition that can be written as:

$$\mathbf{C} = \mathbf{M}^T \Phi \mathbf{M} \quad (7)$$

where  $\mathbf{M}$  is the matrix of orthogonal eigenvectors, which we define to be the force radiation modes ( $f_{\text{rad}}$ -modes). Also,  $\Phi$  is a diagonal matrix whose elements,  $\phi_n$ , are the eigenvalues of  $\mathbf{C}$ . Since the matrix  $\mathbf{C}$  is positive definite, its eigenvalues are all positive and real. Thus the sound power can be written as:

$$\begin{aligned} W &= \mathbf{f}_e^H \mathbf{M}^T \Phi \mathbf{M} \mathbf{f}_e = \mathbf{d}^H \Phi \mathbf{d} \\ &= \sum_{n=1}^N W_n = \sum_{n=1}^N \phi_n |d_n|^2 \end{aligned} \quad (8)$$

where  $\mathbf{d} = \mathbf{M} \mathbf{f}_e$  is the matrix of products of the  $f_{\text{rad}}$ -modes and the driving force distribution. The total radiated sound power when expressed in this way is composed of uncoupled modal radiation powers proportional to the eigenvalues,  $\phi_n$ . Therefore, when the driving force is located at the node of an  $f_{\text{rad}}$ -mode, the sound power radiated by that mode is unequivocally minimized.

## 3 EXPERIMENT

### 3.1 Experimental Setup

While previously the value of  $f_{\text{rad}}$ -mode analysis was demonstrated through simulations, here the objective was to demonstrate that this approach can also be implemented using only experimental data. Figure 1 shows a steel strip which was driven by a transverse force at a point and which consequently radiated sound. The strip was held in a steel frame (i.e., it was clamped at both ends, but not along its edges) and was surrounded by a rigid baffle. The thickness of the strip was 1 mm, the width was 20 mm and the length was 300 mm. The strip was divided into 15 elements of equal length. As shown in Fig. 2, the radiated sound pressure was measured at five points: one was located in the direction normal to the center of the strip, while the other four points were all positioned at an elevation of 45 degrees from the plane of the strip, two being aligned with the strip axis, and two being at right angles to the strip's axis. Further, each point was 1 m from the center of the strip. The radiated sound power was calculated from the average of the mean square sound pressures on the 1 m radius hemispherical surface defined by these five points. The strip itself was driven by a piezoelectric actuator, and the normal velocity of the strip was measured by using an accelerometer to obtain the mobility matrix,  $\mathbf{T}$ . Acoustic transfer functions from

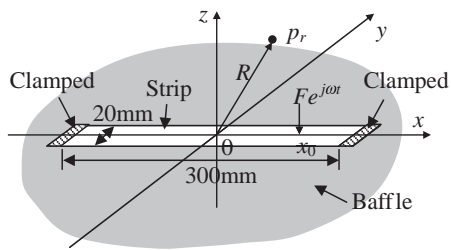
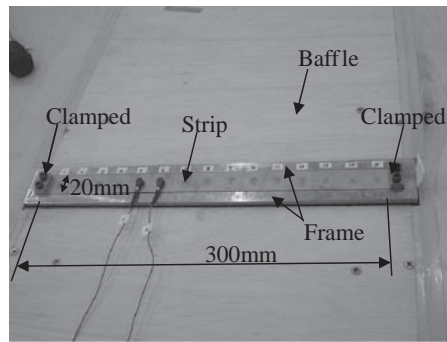


Fig. 1—Vibrating object (steel strip).

the surface of the strip to the microphone locations must be measured to obtain the radiation resistance matrix,  $\mathbf{R}$ . In fact, however, as shown in Fig. 3, the acoustic transfer functions were measured by using reciprocity since the volume source was relatively large compared to the element size on the strip. Thus, the volume source was set in sequence at the locations of the microphones shown in Fig. 2, and the corresponding sound pressures were measured at the surface of the strip.

### 3.2 Experimental Results

Figure 4 shows the sound power radiated when the strip was driven at  $x = -0.08$  m. The sound power was calculated both from the directly measured sound pressures and from the sound pressures estimated as the product of the strip's mobility and the acoustic



transfer functions. As shown in the figure, the two sound powers are in good agreement. Therefore, it can be said that the mobility and the acoustic transfer functions were estimated with reasonable accuracy.

Figure 5 shows the relationship between the driving force location and the sound power, and between the driving force location and the average mean square vibration velocity at 250 and 350 Hz. There it can be seen that there is no clear relation between the radiated sound power and the averaged mean square velocity. In particular, there are clear minima in the radiated sound power at certain driving force locations, while there are no corresponding minima in the averaged velocity. Note also that both frequencies considered here are non-resonant, as can be seen in Fig. 4. Non-resonant frequencies were chosen since the  $f_{\text{rad}}$ -mode analysis is particularly useful in the non-resonant case, as noted in Ref. 7. In contrast, when the structure is driven at a resonant frequency, the shape of the first  $f_{\text{rad}}$ -mode corresponds closely to the first contributing vibration mode (i.e., the first eigenvector of  $\mathbf{U}$ , which is the vibration mode that contributes most to the average mean square velocity). Thus, at a resonant frequency, both modal

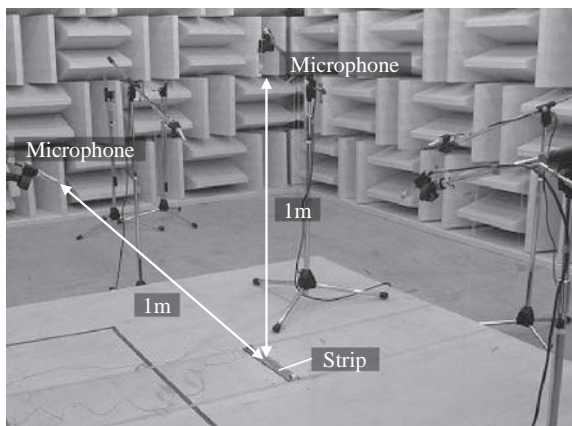
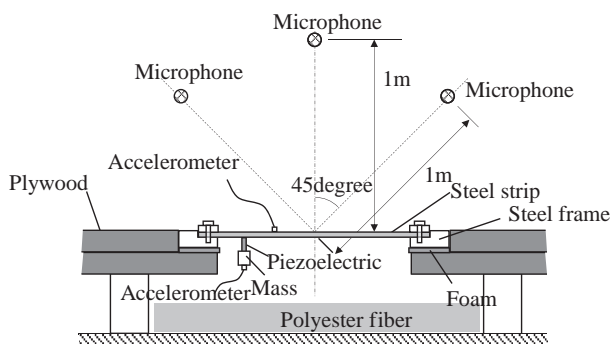


Fig. 2—Experimental setup.

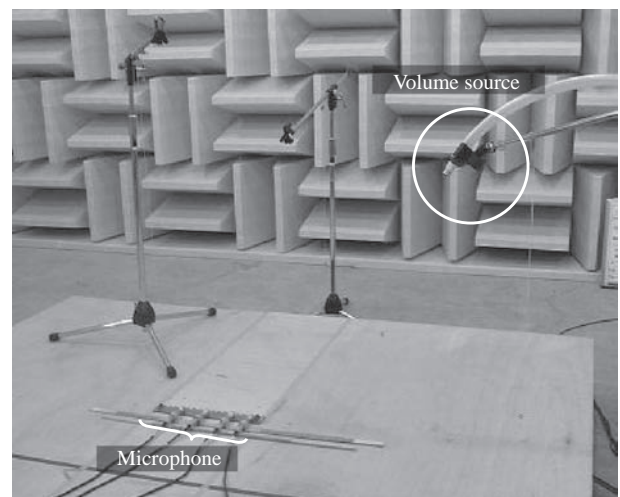


Fig. 3—Measurement of the acoustic transfer functions.



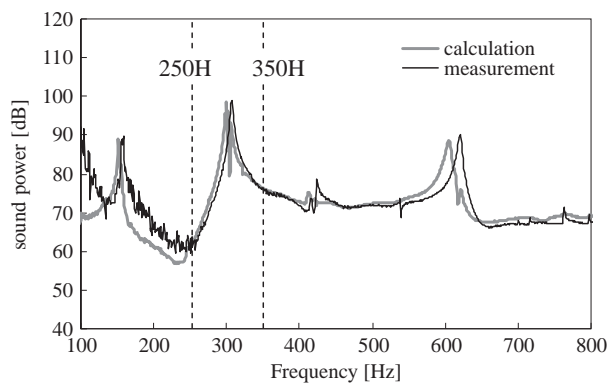


Fig. 4—Comparison between the sound power calculated directly from the measured sound pressures and the sound power calculated from the sound pressures that were estimated from the mobility and the acoustic transfer functions (driven point:  $x = -0.08$  m).

analysis and  $f_{\text{rad}}$ -mode analysis tend to suggest similar solutions, again as noted in Ref. 7.

Figures 6 and 7 show the results of the eigenvalue/eigenvector decompositions of  $\mathbf{U}$ ,  $\mathbf{R}$ , and  $\mathbf{C}$  at 250 and 350 Hz: Figs. 6(a-1) and 7(a-1) show the vibration modes, Figs. 6(b-1) and 7(b-1) show the radiation modes, Figs. 6(c-1) and 7(c-1) show the  $f_{\text{rad}}$ -modes, and plotted in Figs. 6(a-2), 6(b-2) and 6(c-2), and Figs. 7(a-2), 7(b-2) and 7(c-2) are the eigenvalues corresponding to each mode. The eigenvalues of the vibration modes represent their contribution to the mean square vibration velocity averaged over the strip, and the eigenvalues of the  $f_{\text{rad}}$ -modes and the radiation modes represent their contribution to the sound power.

In Fig. 5, it can be seen that the sound power calculated by using the estimated sound pressures is slightly smaller than the sound power calculated directly from the measured sound pressures. However, in general, both agreed well. It can also be seen that the relationship between the driving force location and the sound power is strongly influenced by the first  $f_{\text{rad}}$ -mode. As shown in Fig. 5(a), when the strip was driven near its center at 250 Hz, the radiated sound power was larger than when the strip was driven away from its center: i.e., at a location near the zero-crossing of the first  $f_{\text{rad}}$ -mode. In this case, it can also be seen that the shape of the first  $f_{\text{rad}}$ -mode resulted from the product of the radiation mode and the vibration modes. That is, the shape of the first radiation mode is similar to a superposition of the first contributing vibration mode (that is, the first eigenvector of  $\mathbf{U}$ , which in this case corresponds to the third vibration mode of the beam) and the third contributing vibration mode (i.e.,

the third eigenvector of  $\mathbf{U}$ , whose mode shape corresponds to the first vibration mode of the beam), since both were symmetric, as was the first radiation mode. Therefore the shape of the first  $f_{\text{rad}}$ -mode is similar to the first contributing vibration mode, but the value of the  $f_{\text{rad}}$ -mode at the center of the strip was larger than at other locations on the strip because of the influence of the third contributing vibration mode.

At the same time, as shown in Fig. 5(b), when the strip was driven near its center at 350 Hz, the radiated sound power was relatively small. In particular the sound power is approximately minimized when the first  $f_{\text{rad}}$ -mode crosses zero. The relationship between the driving force location and the sound power was similar to the first  $f_{\text{rad}}$ -mode shown in Fig. 7. The first  $f_{\text{rad}}$ -mode at 350 Hz is also the product of the first radiation mode and the first and the third contributing vibration modes. However, the first contributing vibration mode (the first eigenvector of the  $\mathbf{U}$ , whose mode shape corresponds to the third vibration mode of the beam) has the opposite phase compared to its value at 250 Hz since the third natural frequency lies between 250 and 350 Hz. Therefore, the shapes of the first  $f_{\text{rad}}$ -modes at 250 and 350 Hz are different.

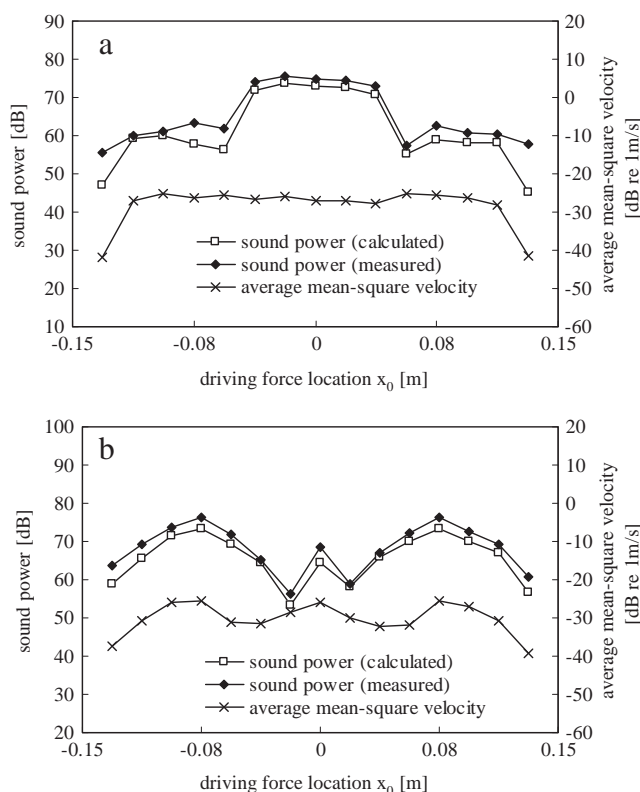


Fig. 5—Relationship between driving force location, the sound power and the average mean square vibration velocity. (a) 250 Hz, (b) 350 Hz.

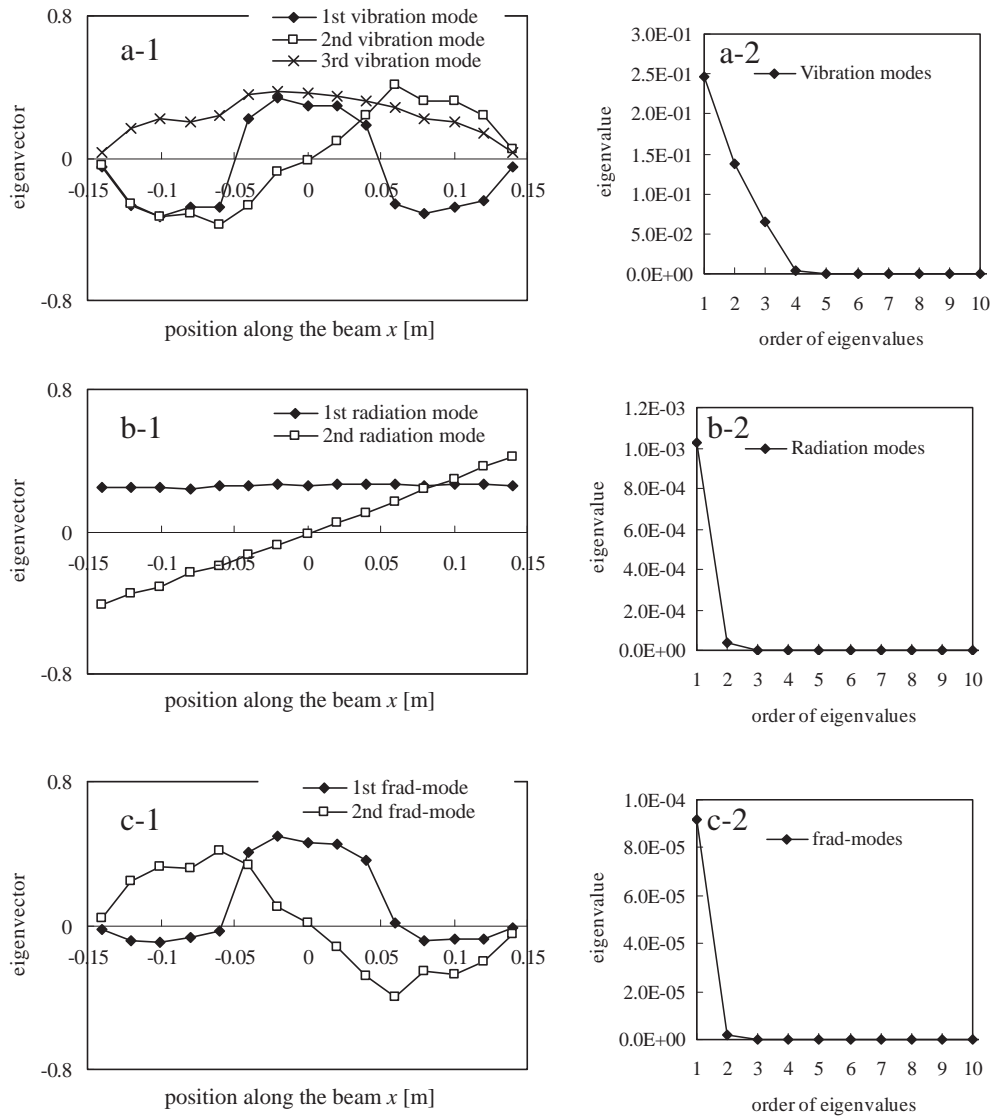


Fig. 6—Eigenvalues and eigenvectors (250 Hz). (a) Vibration modes. (b) Radiation modes. (c)  $f_{rad}$ -modes (left: mode shape, right: eigenvalue). Note that modes are ranked by their contribution at 250 Hz.

In contrast, it is evident that the overall trend of the average mean square vibration velocity was not similar to that of the sound power. The average mean-square velocities at 250 and 350 Hz were almost constant when the strip was driven anywhere except at either end. That behavior results from the fact that the second and third contributing vibration modes contributed significantly to the total vibration (see Figs. 6(a-2) and 7(a-2)).

Note finally that the change in sound power level that results from changing the source location at these frequencies can be as much as 20 dB. In both cases, by locating the vibration source close to the zero-crossing of the  $f_{rad}$ -mode, the radiated sound power is minimized. Thus the results show that the  $f_{rad}$ -modes obtained directly from measured data can provide useful guidance

regarding the driving force locations that result in the minimum sound radiation.

## 4 CONCLUSIONS

In this paper, the acoustic transfer functions and the mobility of a thin steel strip mounted in a rigid baffle were measured to allow the direct calculation of the force radiation modes. It was confirmed that the force radiation modes were identified accurately, and it was also confirmed that the force radiation modes can serve as a practical guide when attempting to reduce the sound power radiated by a vibrating structure.

The force radiation mode concept may be especially useful in the low frequency range when the acoustic power depends on the first few modes, only. The

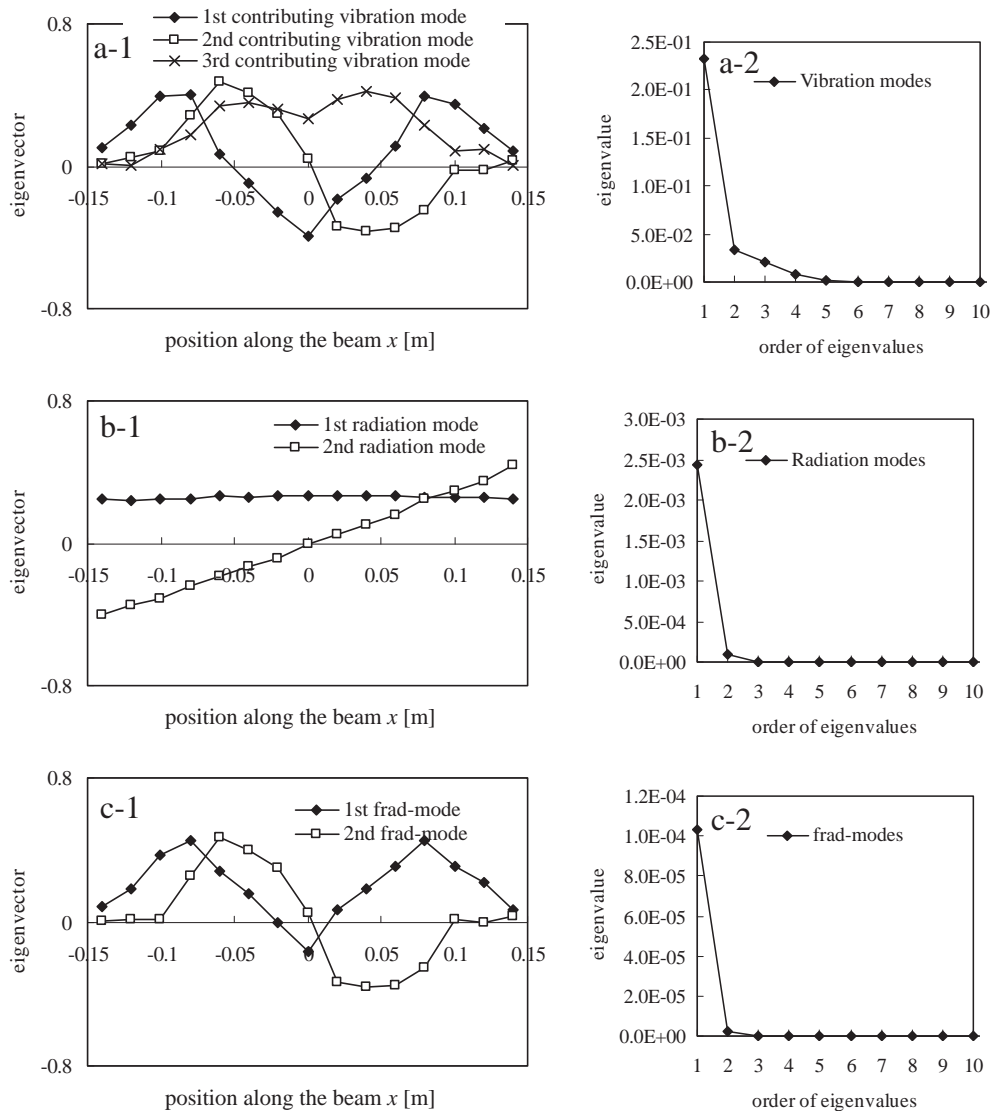


Fig. 7—Eigenvalues and eigenvectors (350 Hz). (a) Vibration modes. (b) Radiation modes. (c)  $f_{rad}$ -modes (left: mode shape, right: eigenvalue). Note that modes are ranked by their contribution at 350 Hz.

reduction of low frequency noise is usually difficult and involves large-scale treatments. Therefore, the reduction of noise simply by changing the vibration source location would be a very useful treatment. In the future, this method will be applied to more complex structures.

## 5 REFERENCES

1. N. Tanaka, Y. Kikushima and M. Kuroda, "Active control of the structure-borne sound", *Japan Society of Mechanical Engineers, Series C*, **57**(541), 62–69, (1991), (in Japanese).
2. J. Pan and C. Bao, "Analytical study of different approaches for active control of sound transmission through double walls", *J. Acoust. Soc. Am.*, **91**(4), 2056–2066, (1992).
3. N. Tanaka and Y. Uchino, "Acoustic power matrix and power mode of a flexible beam", *Japan Society of Mechanical Engineers, Series C*, **66**(648), 106–112, (2000), (in Japanese).
4. S. J. Elliot and M. E. Johnson, "Radiation modes and the active control of acoustic power", *J. Acoust. Soc. Am.*, **94**(4), 2194–2204, (1993).
5. T. Chanpheng, H. Yamada, T. Miyata and H. Katsuchi, "Application of radiation modes to the problem of low-frequency noise from a highway bridge", *Applied Acoustics*, **65**, 109–123, (2004).
6. K. Yum and J. S. Bolton, "Sound radiation modes of a tire on a reflecting surface", *NoiseCon04*, (2004).
7. Z. Yamaguchi, K. Sakagami and J. S. Bolton, "Reduction of sound radiation by using force radiation modes", *Applied Acoustics*, **72**, 420–427, (2011).